Illumina MiSeq reveals the influence of blueberry malvidin-3-galactoside on fecal microbial community structure and metabolizes of liver cancer mice

Zhen Cheng[1], Yuehua Wang[2], Bin Li[1]

[1] College of Food Science, Shenyang Agricultural University, Shenyang, Liaoning, China
[2] College of Food Science, Shenyang Agricultural University, Shenyang, Liaoning, China

Corresponding Author:
Bin Li[1] Dong ling Road, Shen he District, Shenyang, Liaoning, 110866, China
Email address: libinsyau@163.com

Abstract

Hepatocellular carcinoma (HCC) is a kind of cancer with high incidence and often accompanied by intestinal flora imbalance. Many studies have shown that probiotics such as anthocyanins can regulate gut microbiome and improve disease. This study was designed to evaluate the influence of malvidin-3-galactoside (M3G), a blueberry ingredient with several beneficial properties, on gut microorganisms of liver cancer (LC) mice. LC mice were fed M3G diets (LM, 40 mg/kg; HM, 80 mg/kg) or 5-fluorouracil (PC, 20 mg/kg) for three weeks. High-throughput sequencing using the MiSeq platform coupled with freely-available computational tools adopt 16SrRNA and metagenome analyses. There was a greater abundance of *Verrucomicrobiaceae* ($p < 0.05$) and *Ruminococcus* ($p < 0.05$) in mice in the HM group than in those in the LM group. Anti-inflammatory bacteria such as *Akkermansia*, *Sutterella* increase in abundance after fed with M3G for three weeks. A significantly smaller abundance of Proinflammatory bacteria such as *Dorea*, *Coprobacillus*, *Clostridium*, *Streptococcus*, *Oscillospira* in HM mice($p<0.01$). Both M3G and chemotherapeutic drugs can increase signal transduction, Membrane transport, and Cell Motility. In addition, the ability of cell growth and death increased in HM and PC groups but decreased in LC and LM groups. This study indicates that M3G supplementation for three weeks may not be enough to cure liver cancer. However, M3G-supplementation was associated with significant

differences in the structure and metabolic function of gut microbiome compared to liver cancer controls that merit further research.

Subjects Agricultural Science, Food science and technology, Microbiology

Keywords malvidin-3-galactoside, liver cancer, High-throughput sequencing, Fecal microbiota, gut

Introduction

Liver cancer is common cancer in China and age-specific incidence and mortality increased greatly with age (*Zuo et al., 2015*). liver cancer seriously threatens human health and both at home or abroad, the diagnosis and treatment method according to the FTIR spectroscopy, chemotherapy, hepatectomy, radioembolization et currently (*Sheng et al., 2015*; *Mokdad, 2016*).

In recent years, the microbiome has got an increasing concern due to its effect on host metabolism. Indicate human gut microbiota develops with Host and plays a significant role in health and disease (*Wang et al., 2017*). For instance, overwhelming evidence has been published showing a connection between liver cancer and changes in gut microbiome and its metabolism of dietary or Prebiotics(*Ma et al., 2018; Ridlon et al., 2014*; *Qin et al., 2018*; *Fatima, Akhtar & Sheikh, 2017*). Interestingly, intestinal microbiome in patients with liver cancer can be reversed by dietary or probiotic regulation (*Bubnov et al., 2015*). Therefore, the study of the special relationship between functional foods and gut microbiome contributes to the treatment of liver cancer.

Mounting evidence suggests that bioactive substances in food or dietary supplements such as anthocyanins, polyphenols, polysaccharides, probiotics can regulate human gut microbiome and improve intestinal health (*Esposito et al., 2015*; *Ozdal et al., 2016*; *Porter & Martens, 2017*; *Lee et al., 2018*). M3G has been proven to have beneficial functions such as antioxidant (*Huang et al., 2016*), anti-inflammatory (*Huang et al., 2014*), and is part of the human healthy diet *(Skates et al., 2018*). Although many studies have confirmed the functional benefits of Blueberry M3G (*Ma et al., 2018b*), to date there is not enough evidence to support the impact of blueberry M3G on gut microbiome, especially in patients with liver cancer. Regulate the composition structure and metabolic function of the gut microbiome in patients with liver cancer, or as part of therapy to treat liver cancer. Here we show that a 3-week consumption period of an M3G diet did significantly alter gut microbiome structure and metabolize in liver cancer mice. Overall, the composition and metabolic capacity on the gut microbiome of M3G-regulated mice showed an

opposite trend to the LC group in some way. The effect of M3G was mainly concentrated on the gut concentrations of *Akkermansia* and *Ruminococcus* or some trace bacteria genus such as *Lactobacillus*. Metabolic function changes in signal transduction, Membrane transport, and Cell Motility of bacteria were investigated. The results may have implications in the treatment of liver cancer using blueberry M3G.

Materials & Methods

experimental design

The Ethics Animal Use Committee from Shenyang Agricultural University approved all experimental procedures, China. Twenty-four nude male mice were used in this study, Animals were purchased at 6-8-week of age and subcutaneous injection HepG2 cells. liver cancer mice fed with food and water provided ad lib throughout the research. A week later, 24 mice were randomly divided into 4 groups (n = 6 each). mice were designated the Control group (LC, liver cancer mice); the Low-dose blueberry M3G group (LM; 40mg/kg); the High-dose blueberry M3G group (HM; 80mg/kg) and the Positive control group (PC; 5-fluorouracil 20mg/kg). six mice per cage were shut in an environment-controlled room and all mice were health status inspected every day. Represent the first week, the second week and the third week with 0,1,2 and six repetitions are represented by numbers 1-6.

Fecal collection and DNA extraction

After randomized grouping, the feces of each group were collected on the seventh, fourteenth and twenty-first days respectively. The collected feces were frozen in a refrigerator with a sterile centrifuge tube at minus 80 degrees to 16S rRNA gene profiling and metagenome analysis. A suitable method was used to extract DNA from feces samples of liver cancer mice, and the size of the DNA molecule was determined by agar gel electrophoresis of 0.8%. Later, quantification was carried out by ultraviolet spectrophotometer to prepare for amplification. All on-line sequencing was carried out in Shanghai Personal Biotechnology Co., Ltd.

Amplification of different regions of bacterial 16SrRNA by PCR

Ribosomal RNA contains various conserved and variable regions. Conserved regions are used to design primers to amplify single or multiple variable regions of rRNA gene, so that sequence and analyze microbial diversity. Owing to the limitation of MiSeq sequence reading length and the quality of sequencing, the best insertion range is 200-420 bp. In this experiment, a highly variable V4 region of the bacterial 16S rRNA gene of about 250 bp in length was used for

sequencing. PCR amplification using bacteria 16S rDNA V4 region-specific primer, 520F (5'-barcode+ AYTGGGYDTAAAGNG-3'), 802R (5'-TACNVGGGTATCTAATCC-3'). The barcode in the preceding primer is a seven-base oligonucleotide sequence used to distinguishing different samples from the same library. NEB Q5 DNA High Fidelity Polymerase for PCR Amplification. The results were analyzed by 2% agarose gel electrophoresis, and the target fragments were cut. Then the target fragments were recovered by Axygen gel Recovery Kit.

Quantitative and Mixed Samples of PCR Products

Quant-iT PicoGreen dsDNA Assay Kit was used to quantify the PCR products on a Microplate reader (BioTek, FLx800), and then mix the samples according to the amount of data required for each sample.

Library Construction, Quality inspection, and sequencing

This process is based on Illumina's TruSeq Nano DNA LT Library Prep Kit. The first end-repair process is to remove the prominent base at the 5'end of DNA by using End Repair Mix 2 in the kit, complete the missing base at the 3' end, and add a phosphoric acid group at the 5'end. In this process, a single A base is added to the 3'end of DNA to prevent the self-connection of DNA fragments and to ensure that DNA is connected to a sequencing junction with a prominent T base at the 3' end. A specific tagged interface is added to allow DNA to eventually be hybridized to Flow Cell. The DNA fragments of the joints were amplified by PCR, and then the PCR system was purified by BECKMAN AMPure XP beads. The final fragments were selected and purified by 2% agarose gel electrophoresis. Qualified libraries should be calculated at a concentration of more than 2nM. Mixed libraries were transformed into single-stranded libraries by 0.1N NaOH for computer sequencing.

16SrRNA Bacterial Prediction and Metagenome Metabolic Analysis

QIIME software was used to merge and classify the obtained sequences according to 97% sequence similarity and remove rare OUT. Use R software to calculate the total number of OTUs in each sample (group) and present them intuitively through the Venn diagram. Using QIIME software, the composition and abundance distribution tables of each sample at the level of family and genus were obtained, and the analysis results were presented by the histogram. Using soap. coverage to get the protein depths represented by each sequence. The non-redundant protein sequence sets were compared with common protein databases to annotate and analyze the gene functions in each sample. By comparing the protein sequence with the KEGG metabolic pathway

database, the predicted genes of the metagenome can be annotated and classified according to the metabolic pathway.

Statistical analysis

Statistical analysis of data in experiments using statistical methods in high-throughput sequencing. R (ResHacker) software and QIME make data into graphics that can be used to analyze differences intuitively. Using Mothur software and Metastats *(White, Nagarajan & Pop, 2009*) statistical algorithm, the difference of bacterial level between samples was analyzed. Adonis/PERMANOVA analysis gave P values to indicate whether the differences between groups had statistical significance, and 999 substitution tests were conducted to determine whether the differences between groups had statistical significance. P value ($p < 0.001$) reflects the statistical significance of ANOSIM (*Warton, Wright & Wang, 2012*) analysis results.

Results

Common and Special OTU Analysis

The common and special OTU in each group can be clearly observed from Figure 1(A-D) after three weeks. Three weeks after fed with LM3G to liver cancer mice, the total OTU increased from 1507 to 1625. The unique OTUs of LC, LM, and PC increased by 324, 109 and 129 respectively. The study found that the total OTU growth of three groups over time, and there was no significant difference between LM and PC groups. Total OTU dropped from 1756 to 1731 three weeks after fed with HM3G. The unique OTUs in the LC group decreased by 160, while those in HM and PC group increased by 220 and 228. It was concluded that the diversity of gut microbiome in mice with liver cancer gradually decreased with the development of the disease. Anticancer drugs also increase the number of OTUs and the effect likeness to M3G. The experiment proved HM had a greater effect on the number of OTU than LM and increased the diversity of the gut microbiome.

M3G regulates the structure of gut microbiome

Fig. 2-5 showed the diversification of family and genus levels of the gut microbiome in mice with liver cancer after L/HM3G treatment for 3 weeks. At the family level (Fig. 2-3), the main family changed from *S24-7*, *Bacteroidaceae* and *Unclassified Clostridiales* to *S24-7*, *Unclassified Clostridiales,* and *Verrucomicrobiaceae* and the abundance changed from 31.8%, 20.3%, 17.3% to 33.6%, 21.5 %, 17.1%. The total abundance of *Bacteroidaceae* decreased from 20.3% to 9.5%, suggesting that liver cancer could reduce the proportion of *Bacteroidaceae* in the

gut of mice. It was remarkable that the family *S24-7* from *Bacteroides* still occupies the dominant position. *S24-7* is a very rich family of microorganisms in the gut of mice, accounting for half of the gut microbiome, mainly responsible for carbohydrate fermentation (*Tropini et al., 2018*). In comparison, the abundance of *S24-7* in LC and PC groups decreased gradually, while LM and HM increased *S24-7* by 9% and 10% respectively. On the face of it, the effect of HM on this family is better than that of LM, as well as the degree of change of microbiome structure was great before and after the treatment. *Verrucomicrobiaceae* was the dominant family from eleventh to second place, and *Akkwemansia* from this family is beneficial to obese patients (*Sheng et al., 2018*). In the first week, the abundance of the family was low in all groups, about 0.9%. The abundance of the bacteria in the LM group was 4%, and two samples in the HM group were about 30% after 3 weeks. For other samples, it can be attributed to individual differences, but it may be considered that HM is better than LM in improving this family. The abundance of dominant *Bacteroidaceae* decreased by 20%, 11%, 8% and 5% in LC, LM, HM and PC groups, respectively. Therefore, HM and PC could slow down the decline of this family. At the genus level (Fig. 4-5), we observed that after M3G regulation, the abundance of *Bacteroides*, *Lactobacillus* (*Nash et al., 2018*) and harmful bacteria *Dorea* decreased (*Nie et al., 2019*), while the abundance of anti-inflammatory (*van den Munckhof et al., 2018*) bacteria such as *Akkermansia*, *Sutterella,* and *Ruminococcus* increased (*Xu et al., 2018*). It was found that *Ruminococcus* decreased gradually in LC, and LM and HM increased it by about 5%. Chemotherapeutic agents did not have a good regulatory effect on this genus, and the regulating of HM on *Dorea* was better than LM. In conclusion, HM has a better positive regulatory effect on gut microorganisms in liver cancer mice, while 5-F destroys gut homeostasis in mice and reducing the presence of protective genus *(Carvalho et al., 2018*).

Screening of Key Microbial Species

The most significant difference in the intestinal tract of LC mice was *Verrucomicrobiaceae*, *Verrucomicrobiae*, *Akkermansia*, *Verrucomicrobiales,* and *Verrucomicrobiales* after three weeks (Fig. 6). After LM and HM regulation, the dominant species became family and genus of *Bacteroidia* and *Ruminococcaceae*, respectively. Lactobacillaceae, Prevotellaceae, and Lactobacillus. Prevotellaceae are the dominant species with the most significant changes in the PC group. Prevotellaceae was common in the intestinal tract of healthy children (*Pulikkan et al., 2018*), it has also been shown to be associated with obesity (*Li et al., 2018*) and up-regulate three

genes associated with cervical cancer (*Lam et al., 2018*). It was concluded that LM has a better regulation effect on *Bacteroides*, while HM has a more significant effect on *Ruminococcaceae*. Taken together, HM has a greater impact on key microbial species. The microbiome structure regulated by chemotherapeutics was different from M3G, and further research is needed on the causes of the significant changes in *Deferribacteres* in mice with liver cancer.

Hot map analysis of microbiome abundance

Figure 7(A-B) showed cluster thermogram analysis of the top 20 taxa with the most significant difference in abundance. The clustering of gut microbiome abundance after three weeks of LC, LM and PC groups showed at Figure 7A. It was observed that *Lactococcus*, *Coprobacillus*, *Dorea*, *Clostridium*, *Mucisprillum,* and *Streptococcus* clustered in the LC group and accompanied by higher abundance. The microbiome aggregates in a cluster indicated similar nature. For instance, *Dorea* and *Clostridium* are opportunistic pathogens can cause inflammation or obesity *(Le Bastard et al., 2018*), but these species are less abundant in the LM and PC groups, it showed that M3G and 5-F have a good regulatory effect on these harmful bacteria. Figure 7B showed the regulatory effect of HM on gut microbiome in mice with liver cancer. *Oscillospira*, [*Ruminococcus*] and *Lactobacillus* were observed to account for a higher proportion in the HM group. At the same time, HM also regulated the high expression of bacteria in the LC group. Although the abundance of Bacteroides in HM was lower than that in the LM group, M3G increased the abundance of Bacteroides in general. It was concluded that the gut microbiome abundance of liver cancer mice changed greatly after M3G regulation compared with LC and PC groups.

Basic metabolic changes in the gut microbiome

The effect of M3G on gut microbiome metabolism in mice with hepatocellular carcinoma was analyzed by metagenome functional annotation (Fig. 8A-D). Figure 8(A-D) represented the comparison of metabolic functions of LC, LM, HM and PC groups in the first and third weeks, respectively. Human Diseases; Cancers and Environmental Information Processing; Signaling Molecules and Interaction were found to increase with time in all four groups, but the change was not significant. Cellular Community-Prokaryotes metabolic function was significantly increased in liver cancer mice, but not elevated in other groups. M3G and chemotherapy drugs increase the metabolic capacity of the LC group, such as Signal Transduction, Membrane

Transport, and Cell Motility. However, the metabolic capacity of Cell Growth and Death in the HM and PC groups increased, and the LC and LM groups showed a downward trend.

Discussion

Anthocyanin acts as an inducer of cell rest and death in healthy breast cells through down-regulation of KDM5B in a dose-dependent manner (*Nanashima et al., 2017*)**.** However, the effect of M3G dosage on the gut microbiome of diseased individuals has not been clearly identified. The current study has assessed the structure and function of the gut microbiome in mice with hepatocellular carcinoma under different treatments for three weeks. Our data showed that liver cancer can reduce the diversity of gut microbiome. Different doses of M3G have different effects on the abundance of certain bacteria in the gut microbiome, which may be the cause of different functional changes. 5-fluorouracil could inhibit the abundance of some pathogenic bacteria, but also cause intestinal flora imbalance. These changes in microbiome structure and function may involve deeper aspects, such as individual differences, the transformation between opportunistic pathogens and pathogens, the particularity of the disease itself, and the specificity of M3G. Fundamental molecular mechanisms, such as how M3G reacts with intestinal bacteria or how it acts, have not been fully validated. This requires us to do more research on this basis.

To our knowledge, there are few reports about the regulation of gut microbiome by M3G in liver cancer mice. It has been reported that consumption of blueberries and other berries reduces intestinal oxygen and oxidative stress, resulting in a strong transfer of gastrointestinal bacterial communities to specific anaerobes *(Overall et al., 2017*). The use of gastrointestinal microbial regulators containing blueberry anthocyanins also increased short-chain fatty acids in the intestine and feces, suggesting that the abundance of lipid-metabolizing bacteria in the intestine may increase (*Microbiome, Improves & Trial, 2016*). *Bacteroides*, *Akkermansia*, and *Bifidobacterium spp*. are the main beneficial bacteria associated with lipid metabolism in the gut (*Shen, Gaskins & McIntosh, 2014*). In this study, *Akkermansia* increased over time in the intestines of mice with liver cancer after regulated by M3G for three weeks and the downward trend of *Bacteroides* will also be mitigated. Decreased intestinal flora diversity has been reported to cause *Clostridium* infection and inflammation (*Le Bastard et al., 2018*). Mitochondrial damage in the liver increases the abundance of *Clostridium* in the gut (*Crescenzo et al., 2017*). Liver mitochondria may be damaged in patients with liver cancer as the disease progresses.

Through this study, we can observe that *Clostridium* increases gradually in the LC group, while M3G decreases its abundance, which proves that M3G has a moderating effect on the number of harmful *Clostridium*. The overall difference of gut microbiome in liver cancer mice was not obvious by the dosage of blueberry M3G, but the regulation of some certain flora was relatively different. In conclusion, further research is needed to support the emergence of these phenomena. The different effects of different doses of blueberry M3G on intestinal microorganisms in mice with liver cancer can be verified by human clinical research, not only by mouse analysis, in order to more accurately determine the difference between human and animal individuals, which is also the next step we need to plan. It is worth noting how to determine the optimal dosage of blueberry M3G in order to avoid the phenomenon of ineffective or wasteful effects, and the impact of other factors in the study need to be more accurately designed.

The effect of blueberry M3G on gut microbiome may be attributed to the regulation of specific flora abundance and diversity in liver cancer mice. Meanwhile, functional annotations of the metagenomic also showed that blueberry M3G did affect the metabolic function of the flora in mice with hepatocellular carcinoma. Lipid metabolism in liver cancer mice decreased in the LM group but increased in the other three groups. Previous studies have shown that changes in lipid metabolism are associated with the promotion of liver tumors in rats (*Riedel et al., 2015*). Current studies are limited to the determination of physiological indicators and changes in liver tumors in mice to determine the impact of blueberry M3G dosage. Further studies are needed on the dose of blueberry M3G which can treat or regulate liver cancer into healthy intestinal microbiome. Special attention should be paid to individual differences when conducting similar studies again. The next step is to further explore and analyze the changes of metabolic function of blueberry M3G.

Conclusions

Our study demonstrated that both high and low doses of blueberry M3G could positively regulate the structure and diversity of gut microbiome in mice with liver cancer. At the same time, blueberry M3G could alter the metabolic function of the certain gut microbiome, but the degree of regulation was slightly different.

Acknowledgements

Funding

This work was supported by the National Natural Science Foundation of China (31671836), the Innovative Talent Support Program for Institution of Higher Learning of Liaoning Province (LR2017038) and the Young and Middle-aged Technological Innovation Support Program of Shenyang Science and Technology Bureau (RC170247). The funders had no role in study design, data collection, and analysis, decision to publish, or preparation of the manuscript.

Grant Disclosures

The following grant information was disclosed by the authors:

the National Natural Science Foundation of China (31671836), the Innovative Talent Support Program for Institution of Higher Learning of Liaoning Province (LR2017038), the Young and Middle-aged Technological Innovation Support Program of Shenyang Science and Technology Bureau (RC170247).

Competing Interests

The authors declare there are no competing interests.

Author Contributions

• Bin Li, Yuehua Wang, and Yu Xiao conceived and designed the experiments.

• Zhen Cheng analyzed the data, wrote the paper, prepared figures and/or tables.

• The relevant staff of the Army General Hospital carried out experiments and provided reagent/material/analysis tools.

Field Study Permissions

Provide the following information on field research approval (i.e. approval bodies and any reference numbers):

All the experiments were approved by the Ethics Committee of Shenyang Agricultural University.

References

Bubnov R V., Spivak MY, Lazarenko LM, Bomba A, Boyko N V. 2015. Probiotics and immunity: Provisional role for personalized diets and disease prevention. *EPMA Journal* 6:1–11. DOI: 10.1186/s13167-015-0036-0.

Carvalho R, Vaz A, Pereira FL, Dorella F, Aguiar E, Chatel J-M, Bermudez L, Langella P, Fernandes G, Figueiredo H, Goes-Neto A, Azevedo V. 2018. Gut microbiome modulation during treatment of mucositis with the dairy bacterium Lactococcus lactis and recombinant strain secreting human antimicrobial PAP. *Scientific Reports* 8:15072. DOI: 10.1038/s41598-018-33469-w.

Crescenzo R, Mazzoli A, Di Luccia B, Bianco F, Cancelliere R, Cigliano L, Liverini G, Baccigalupi L, Iossa S. 2017. Dietary fructose causes defective insulin signaling and

ceramide accumulation in the liver that can be reversed by gut microbiota modulation. *Food and Nutrition Research* 61. DOI: 10.1080/16546628.2017.1331657.

Esposito D, Damsud T, Wilson M, Grace MH, Strauch R, Li X, Lila MA, Komarnytsky S. 2015. Black Currant Anthocyanins Attenuate Weight Gain and Improve Glucose Metabolism in Diet-Induced Obese Mice with Intact, but Not Disrupted, Gut Microbiome. *Journal of Agricultural and Food Chemistry* 63:6172–6180. DOI: 10.1021/acs.jafc.5b00963.

Fatima N, Akhtar T, Sheikh N. 2017. Prebiotics: A Novel Approach to Treat Hepatocellular Carcinoma. *Canadian Journal of Gastroenterology and Hepatology* 2017. DOI: 10.1155/2017/6238106.

Huang WY, Liu YM, Wang J, Wang XN, Li CY. 2014. Anti-inflammatory effect of the blueberry anthocyanins malvidin-3-glucoside and malvidin-3-galactoside in endothelial cells. *Molecules* 19:12827–12841. DOI: 10.3390/molecules190812827.

Huang W, Zhu Y, Li C, Sui Z, Min W. 2016. Effect of blueberry anthocyanins malvidin and glycosides on the antioxidant properties in endothelial cells. *Oxidative Medicine and Cellular Longevity* 2016. DOI: 10.1155/2016/1591803.

Lam KC, Vyshenska D, Hu J, Rodrigues RR, Nilsen A, Zielke RA, Brown NS, Aarnes E-K, Sikora AE, Shulzhenko N, Lyng H, Morgun A. 2018. Trans-kingdom network reveals bacterial players associated with cervical cancer gene expression program. *PeerJ* 6:e5590. DOI: 10.7717/peerj.5590.

Le Bastard Q, Ward T, Sidiropoulos D, Hillmann BM, Chun CL, Sadowsky MJ, Knights D, Montassier E. 2018. Fecal microbiota transplantation reverses antibiotic and chemotherapy-induced gut dysbiosis in mice. *Scientific Reports* 8:1–11. DOI: 10.1038/s41598-018-24342-x.

Lee E-S, Song E-J, Nam Y-D, Lee S-Y. 2018. Probiotics in human health and disease: from nutribiotics to pharmabiotics. *Journal of Microbiology* 56:773–782. DOI: 10.1007/s12275-018-8293-y.

Li X, Rensing C, Taylor WL, Costello C, Brejnrod AD, Ferry RJ, Higgins PB, Folli F, Kottapalli KR, Hubbard GB, Dick EJ, Yooseph S, Nelson KE, Schlabritz-Loutsevitch N. 2018. *Papio* spp. Colon microbiome and its link to obesity in pregnancy. *Journal of Medical Primatology*:1–9. DOI: 10.1111/jmp.12366.

Ma C, Han M, Heinrich B, Fu Q, Zhang Q, Sandhu M, Agdashian D, Terabe M, Berzofsky JA, Fako V, Ritz T, Longerich T, Theriot CM, McCulloch JA, Roy S, Yuan W, Thovarai V, Sen SK, Ruchirawat M, Korangy F, Wang XW, Trinchieri G, Greten TF. 2018a. Gut microbiome–mediated bile acid metabolism regulates liver cancer via NKT cells. *Science* 360. DOI: 10.1126/science.aan5931.

Ma L, Sun Z, Zeng Y, Luo M, Yang J. 2018b. Molecular mechanism and health role of functional ingredients in blueberry for chronic disease in human beings. *International Journal of Molecular Sciences* 19. DOI: 10.3390/ijms19092785.

Microbiome G, Improves M, Trial CP. 2016. HHS Public Access. 29:1272–1276. DOI: 10.1016/j.jdiacomp.2015.08.023.Gastrointestinal.

Mokdad AA. 2016. Treatment of liver cancer. *Journal of the American Medical Association* 315:100. DOI: 10.1001/jama.2015.15431.

van den Munckhof ICL, Kurilshikov A, Ter Horst R, Riksen NP, Joosten LAB, Zhernakova A, Fu J, Keating ST, Netea MG, de Graaf J, Rutten JHW. 2018. Role of gut microbiota in chronic low-grade inflammation as a potential driver for atherosclerotic cardiovascular

disease: a systematic review of human studies. *Obesity Reviews*:1719–1734. DOI: 10.1111/obr.12750.

Nanashima N, Horie K, Chiba M, Nakano M, Maeda H, Nakamura T. 2017. Anthocyanin-rich blackcurrant extract inhibits proliferation of the MCF10A healthy human breast epithelial cell line through induction of G0/G1 arrest and apoptosis. *Molecular Medicine Reports* 16:6134–6141. DOI: 10.3892/mmr.2017.7391.

Nash V, Ranadheera CS, Georgousopoulou EN, Mellor DD, Panagiotakos DB, McKune AJ, Kellett J, Naumovski N. 2018. The effects of grape and red wine polyphenols on gut microbiota – A systematic review. *Food Research International* 113:277–287. DOI: 10.1016/j.foodres.2018.07.019.

Nie Q, Hu J, Gao H, Fan L, Chen H, Nie S. 2019. Polysaccharide from Plantago Asiatica L. attenuates hyperglycemia, hyperlipidemia and affects colon microbiota in type 2 diabetic rats. *Food Hydrocolloids* 86 34–42. DOI: 10.1016/j.foodhyd.2017.12.026.

Overall J, Bonney SA, Wilson M, Beermann A, Grace MH, Esposito D, Lila MA, Komarnytsky S. 2017. Metabolic effects of berries with structurally diverse anthocyanins. *International Journal of Molecular Sciences* 18. DOI: 10.3390/ijms18020422.

Ozdal T, Sela DA, Xiao J, Boyacioglu D, Chen F, Capanoglu E. 2016. The reciprocal interactions between polyphenols and gut microbiota and effects on bioaccessibility. *Nutrients* 8:1–36. DOI: 10.3390/nu8020078.

Porter NT, Martens EC. 2017. The Critical Roles of Polysaccharides in Gut Microbial Ecology and Physiology. *Annual Review of Microbiology* 71:349–369. DOI: 10.1146/annurev-micro-102215-095316.

Pulikkan J, Maji A, Dhakan DB, Saxena R, Mohan B, Anto MM, Agarwal N, Grace T, Sharma VK. 2018. Gut Microbial Dysbiosis in Indian Children with Autism Spectrum Disorders. *Microbial Ecology*:1–13. DOI: 10.1007/s00248-018-1176-2.

Qin Y, Roberts JD, Grimm SA, Lih FB, Deterding LJ, Li R, Chrysovergis K, Wade PA. 2018. An obesity-associated gut microbiome reprograms the intestinal epigenome and leads to altered colonic gene expression. *Genome Biology* 19:1–14. DOI: 10.1186/s13059-018-1389-1.

Ridlon JM, Kang DJ, Hylemon PB, Bajaj JS. 2014. Bile acids and the gut microbiome. *Current Opinion in Gastroenterology* 30:332–338. DOI: 10.1097/MOG.0000000000000057.

Riedel S, Abel S, Swanevelder S, Gelderblom WCA. 2015. Induction of an altered lipid phenotype by two cancer-promoting treatments in rat liver. *Food and Chemical Toxicology* 78:96–104. DOI: 10.1016/j.fct.2015.01.023.

Shen W, Gaskins HR, McIntosh MK. 2014. Influence of dietary fat on intestinal microbes, inflammation, barrier function, and metabolic outcomes. *Journal of Nutritional Biochemistry* 25:270–280. DOI: 10.1016/j.jnutbio.2013.09.009.

Sheng L, Jena PK, Liu H-X, Hu Y, Nagar N, Bronner DN, Settles ML, Bäumler AJ, Wan Y-JY. 2018. Obesity treatment by epigallocatechin-3-gallate–regulated bile acid signaling and its enriched *Akkermansia muciniphila*. *The FASEB Journal*:fj.201800370R. DOI: 10.1096/fj.201800370R.

Sheng D, Xu F, Yu Q, Fang T, Xia J, Li S, Wang X. 2015. A study of structural differences between liver cancer cells and normal liver cells using FTIR spectroscopy. *Journal of Molecular Structure* 1099:18–23. DOI: 10.1016/j.molstruc.2015.05.054.

Skates E, Overall J, DeZego K, Wilson M, Esposito D, Lila MA, Komarnytsky S. 2018. Berries containing anthocyanins with enhanced methylation profiles are more effective at

ameliorating high fat diet-induced metabolic damage. *Food and Chemical Toxicology* 111:445–453. DOI: 10.1016/j.fct.2017.11.032.

Tropini C, Moss EL, Merrill BD, Ng KM, Higginbottom SK, Casavant EP, Gonzalez CG, Fremin B, Bouley DM, Elias JE, Bhatt AS, Huang KC, Sonnenburg JL. 2018. Transient Osmotic Perturbation Causes Long-Term Alteration to the Gut Microbiota. *Cell* 173:1742–1754.e17. DOI: 10.1016/j.cell.2018.05.008.

Wang Y, Wang B, Wu J, Jiang X, Tang H, Nielsen OH. 2017. Modulation of Gut Microbiota in the Pathological States. *Engineering* 3:83–89. DOI: 10.1016/J.ENG.2017.01.013.

Warton DI, Wright ST, Wang Y. 2012. Distance-based multivariate analyses confound location and dispersion effects. *Methods in Ecology and Evolution* 3:89–101. DOI: 10.1111/j.2041-210X.2011.00127.x.

White JR, Nagarajan N, Pop M. 2009. Statistical Methods for Detecting Differentially Abundant Features in Clinical Metagenomic Samples. *PLoS Computational Biology* 5. DOI: 10.1371/journal.pcbi.1000352.

Xu H, Wei Y, Ma H, Liu Y, Zhang Y, Hu L, Li J. 2018. Alterations of Gut Microbiome in the Patients With Severe Fever With Thrombocytopenia Syndrome. *Frontiers in Microbiology* 9:1–9. DOI: 10.3389/fmicb.2018.02315.

Zuo TT, Zheng RS, Zhang SW, Zeng HM, Chen WQ. 2015. Incidence and mortality of liver cancer in China in 2011. *Chinese Journal of Cancer* 34:1–6. DOI: 10.1186/s40880-015-0056-0.

Figure 1
Venn diagram analysis
(A)Number of shared and unique OTUs in LC, LM and PC groups during the first week
(B)Number of shared and unique OTUs in LC, LM and PC groups during the third week
(C)Number of shared and unique OTUs in LC, HM and PC groups during the first week
(D)The number of shared and unique OTUs in LC, HM and PC groups during the third week

Figure 2
Comparative analysis of family-level colonies in LM group
(A)Comparisons of LM with LC and PC in the first week
(B)Comparisons of LM with LC and PC in the third week

Figure 3
Comparative analysis of family-level colonies in HM group
(A)Comparisons of HM with LC and PC in the first week
(B)Comparisons of HM with LC and PC in the third week

Figure 4
Comparative analysis of genus-level colonies in LM group
(A)Comparisons of LM with LC and PC in the first week
(B)Comparisons of LM with LC and PC in the third week

Figure 5
Comparative analysis of genus-level colonies in HM group
(A)Comparisons of HM with LC and PC in the first week
(B)Comparisons of HM with LC and PC in the third week

Figure 6
LDA analysis
(A)Comparison of LC, LM and PC
(B)Comparison of LC and HM

Figure 7
Hot-map analysis
(A)Colony Abundance Clustering of LC, LM and PC at the Third Week
(B)Colony Abundance Clustering of LC, HM and PC at the Third Week

Figure 8
Comparative analysis of functional metabolism of gut microbiome
(A)Microbial metabolism in LC group during the third and first week
(B)Microbial metabolism in LM group during the third and first week
(C)Microbial metabolism in HM group during the third and first week
(D)Microbial metabolism in PC group during the third and first week

Figure 1

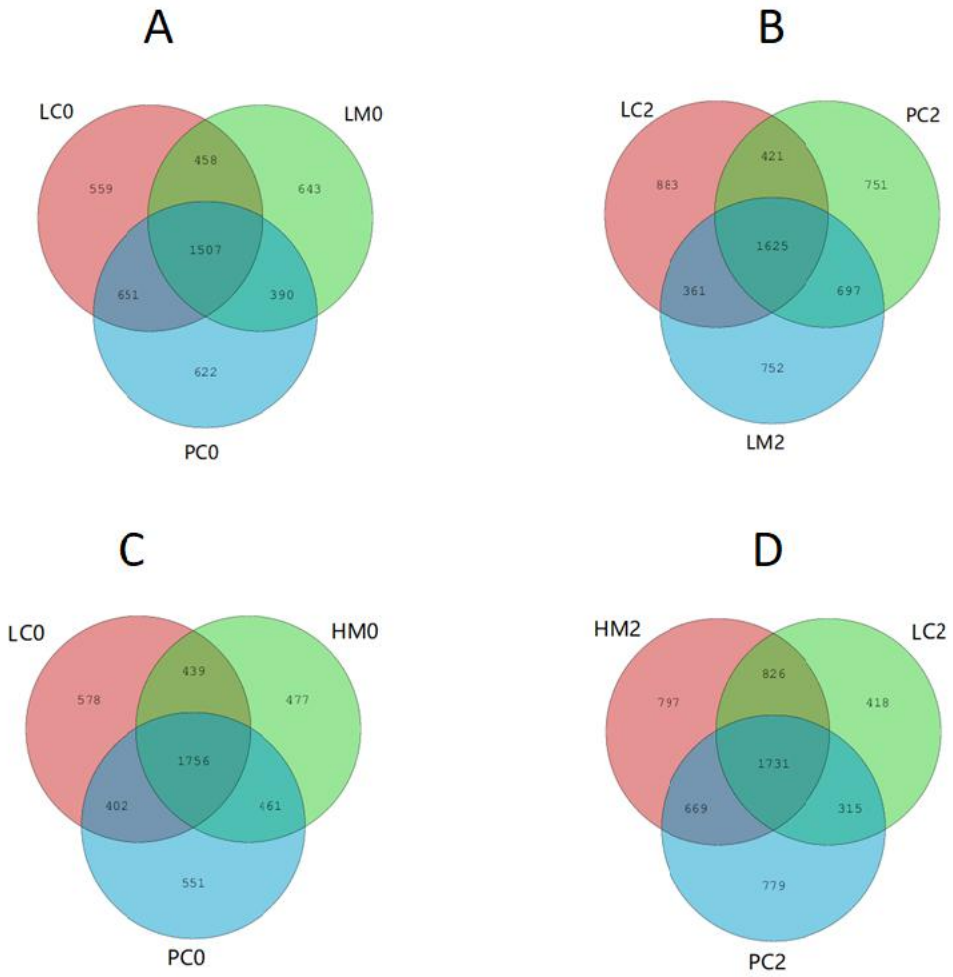
A
LC0
LM0
PC0
559
458
643
1507
651
390
622
B
LC2
PC2
LM2
883
421
751
1625
361
697
752
C
LC0
HM0
PC0
578
439
477
1756
402
461
551
D
HM2
LC2
PC2
797
826
418
1731
669
315
779

513 Figure 2.

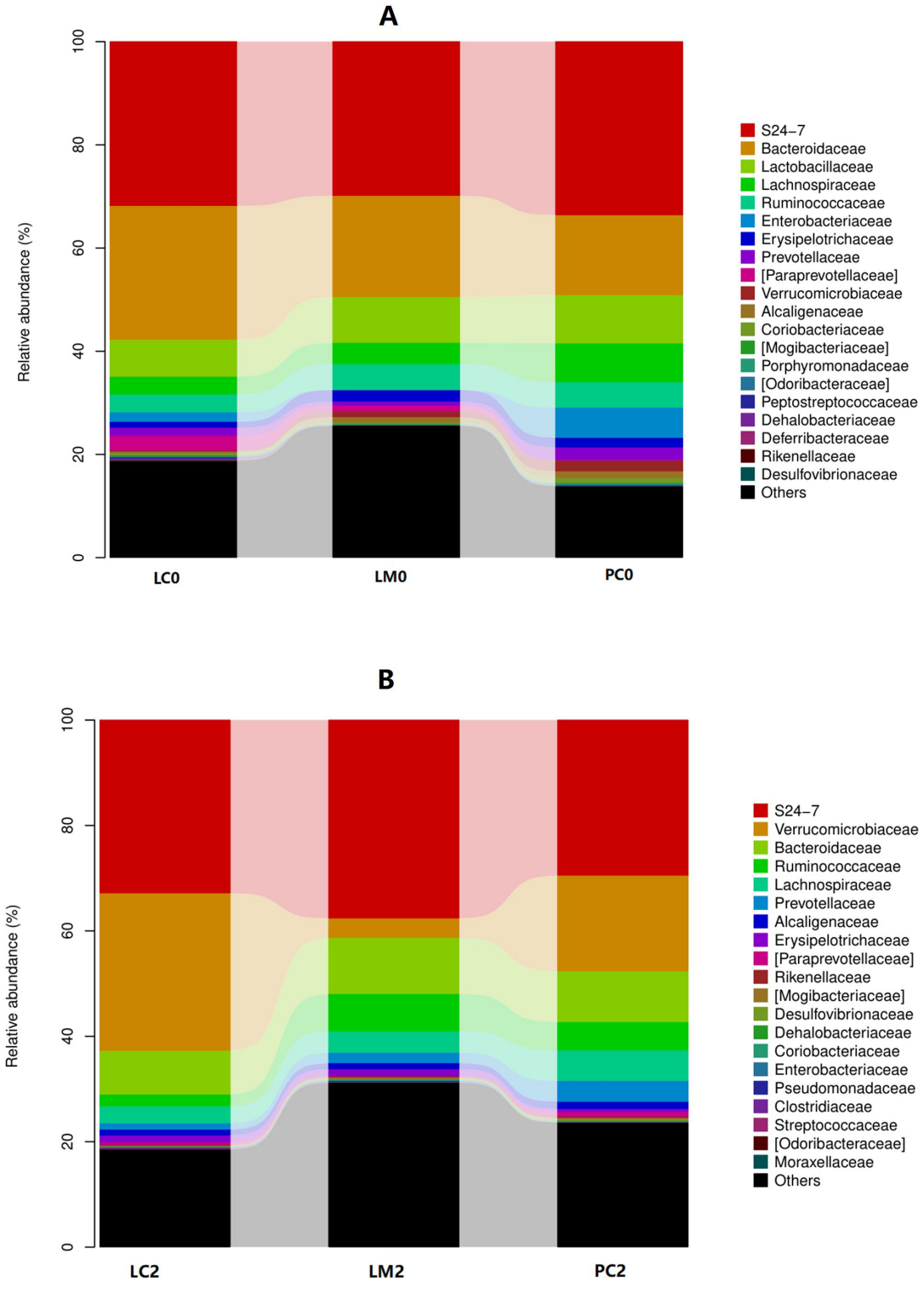

514
515

516 Figure 3.

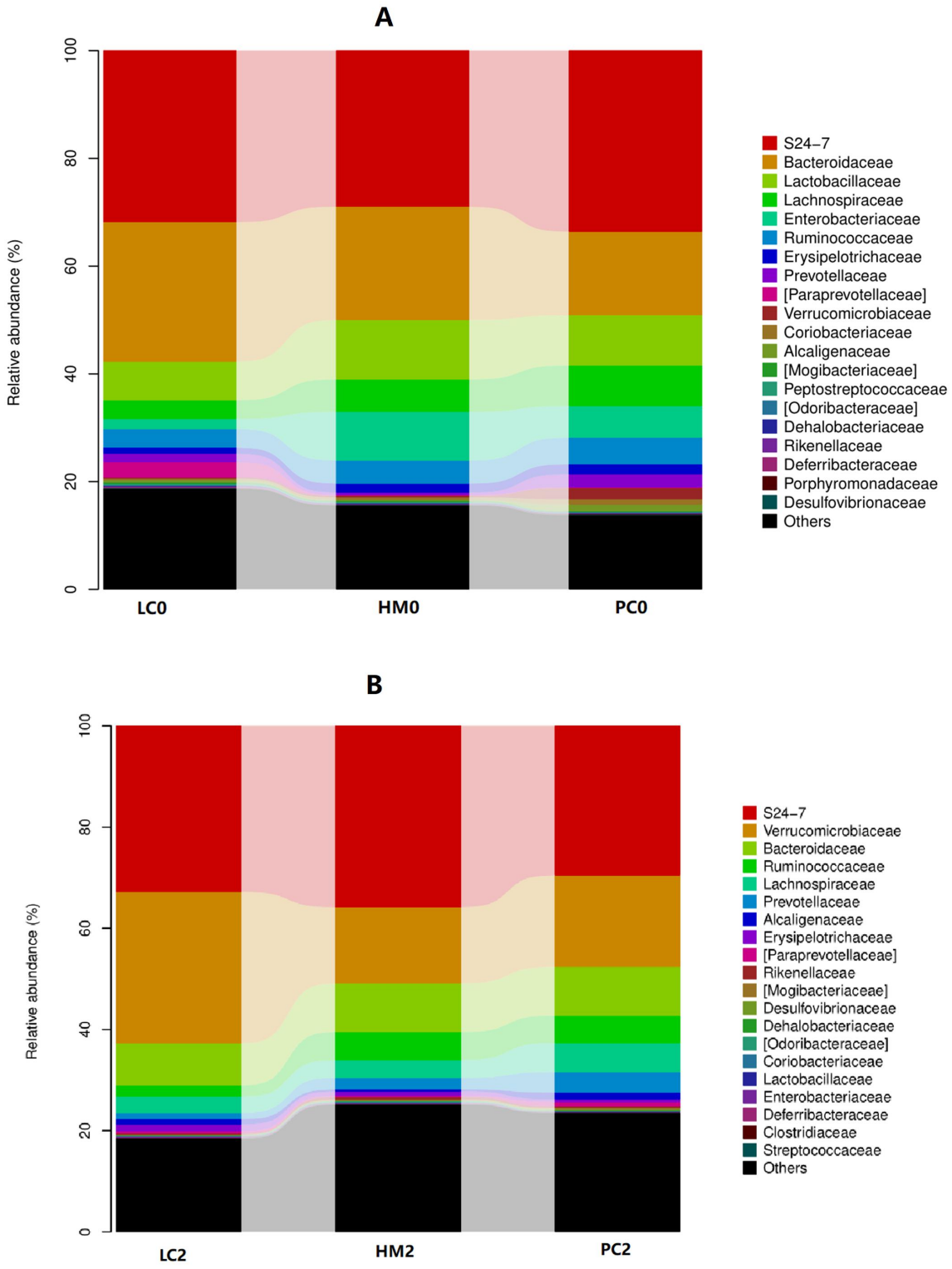

517
518

519 Figure 4.

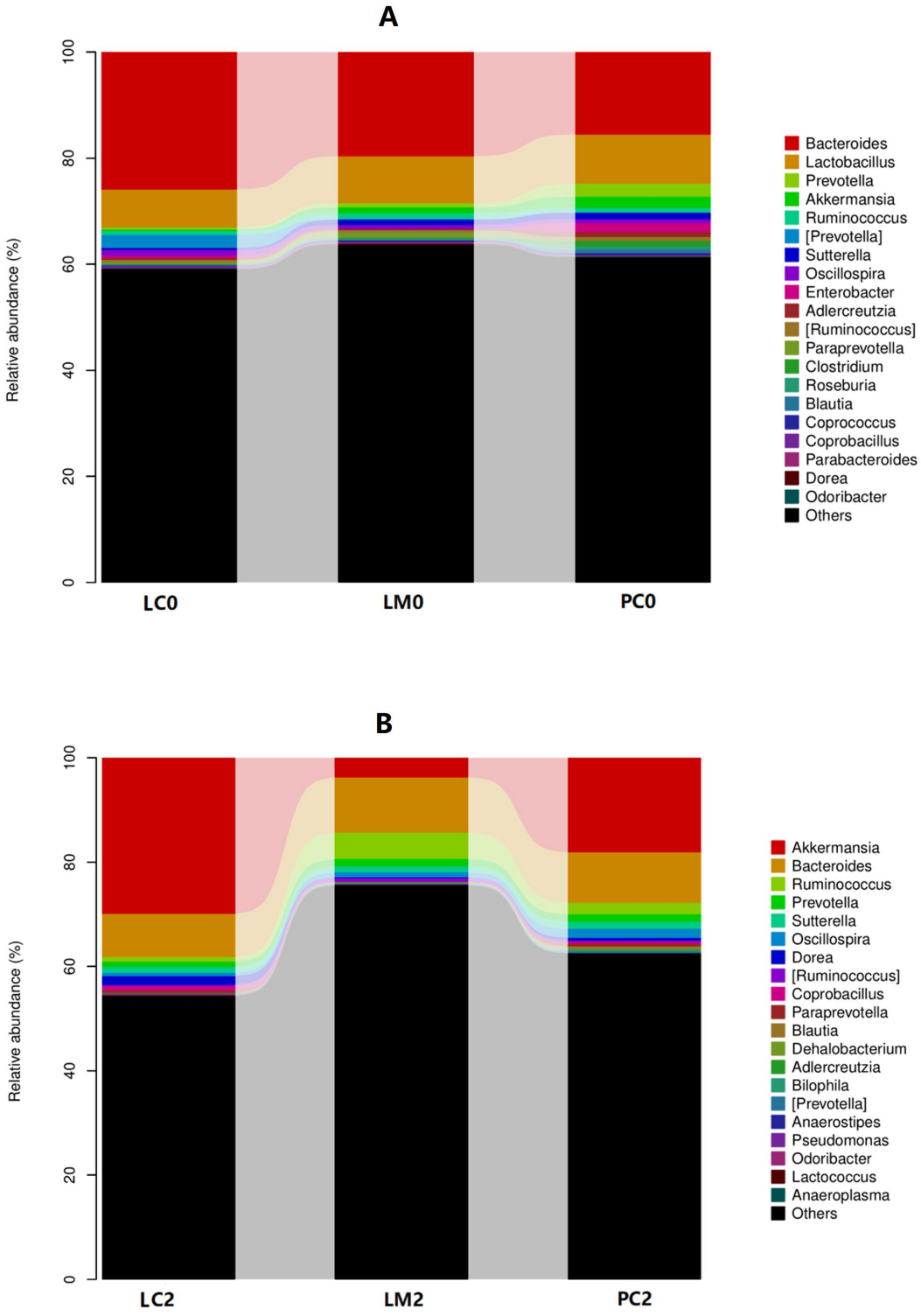

520
521

522 Figure 5.

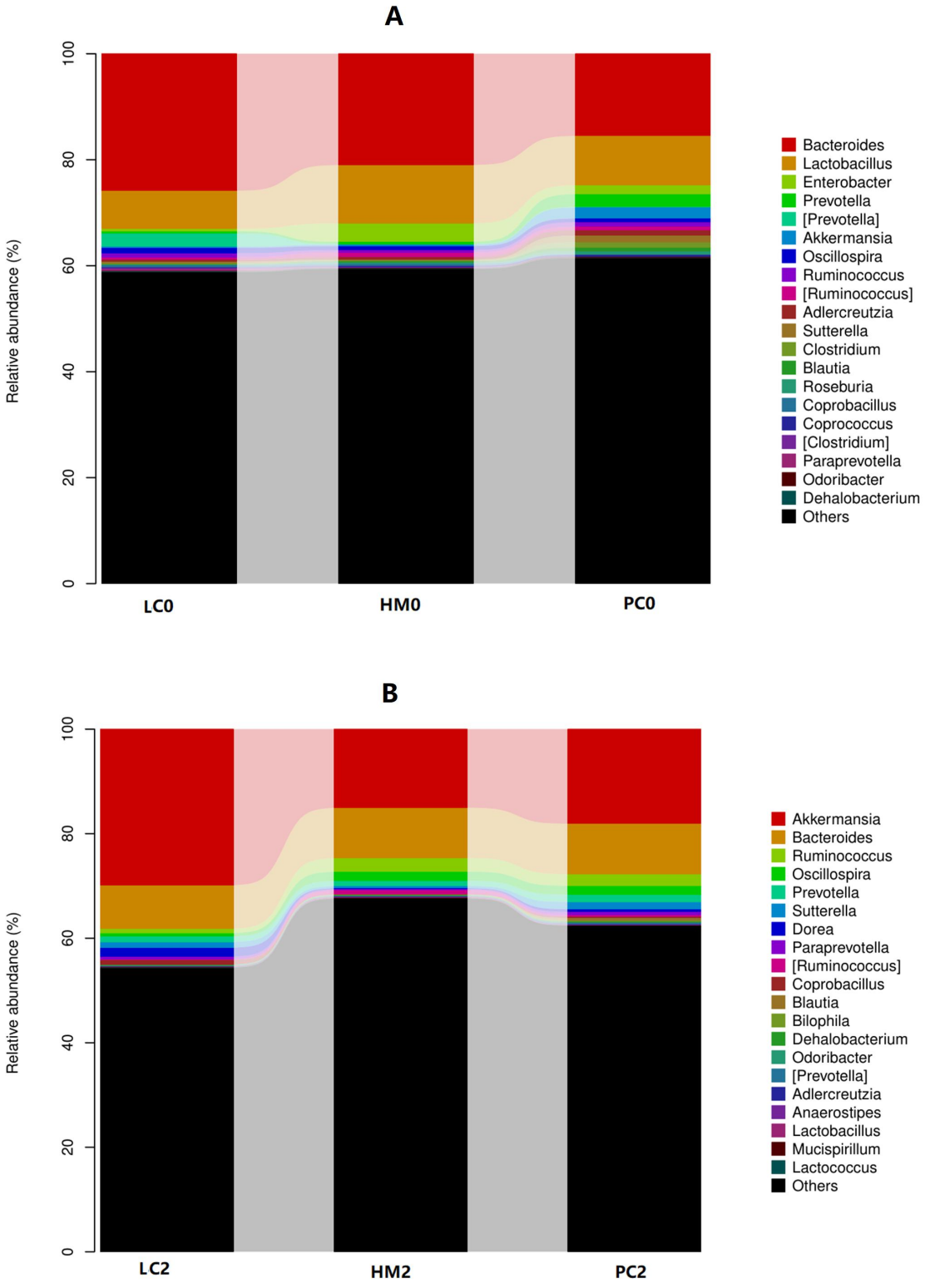

523
524

525 Figure 6.

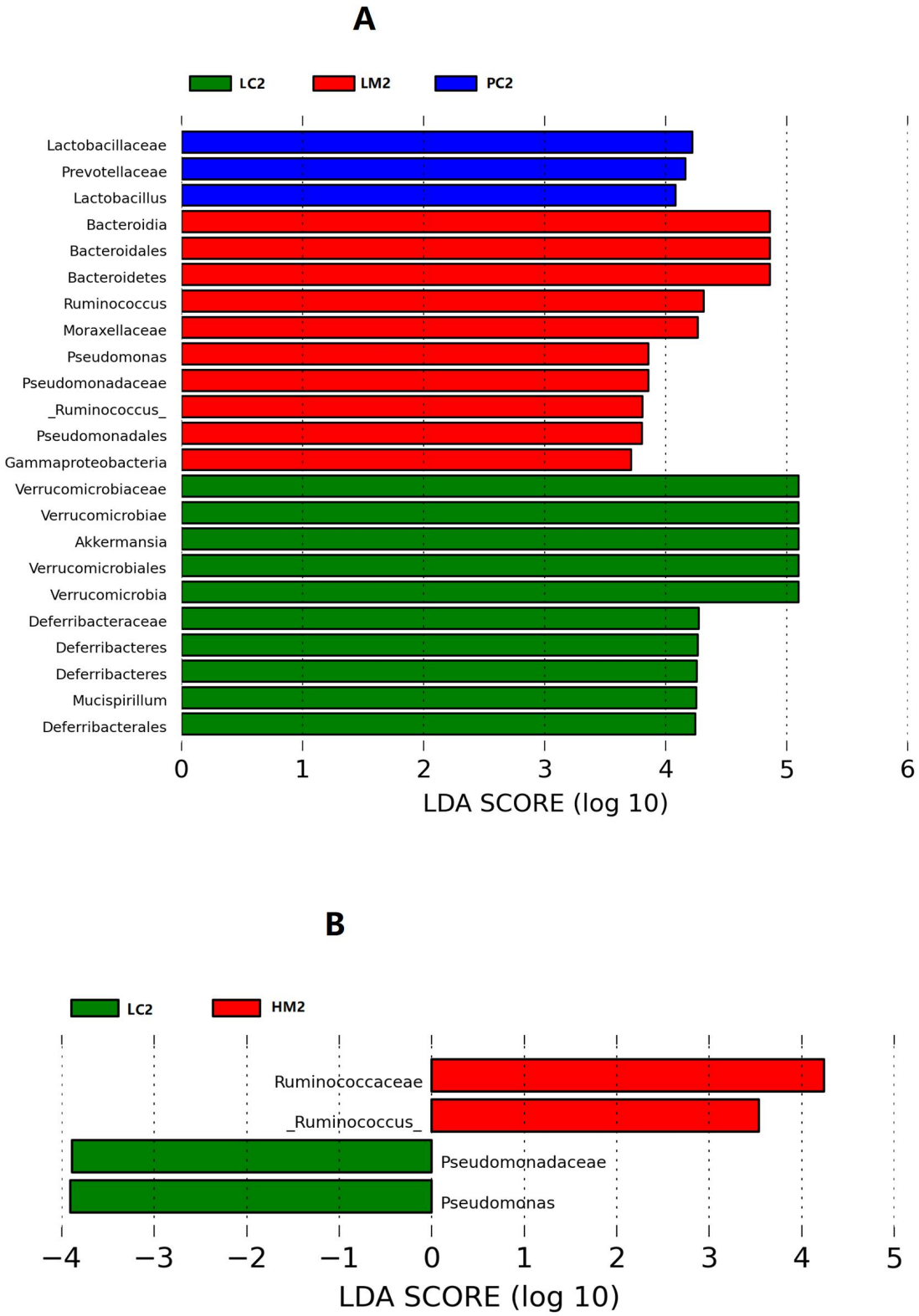

526
527

528 Figure 7.

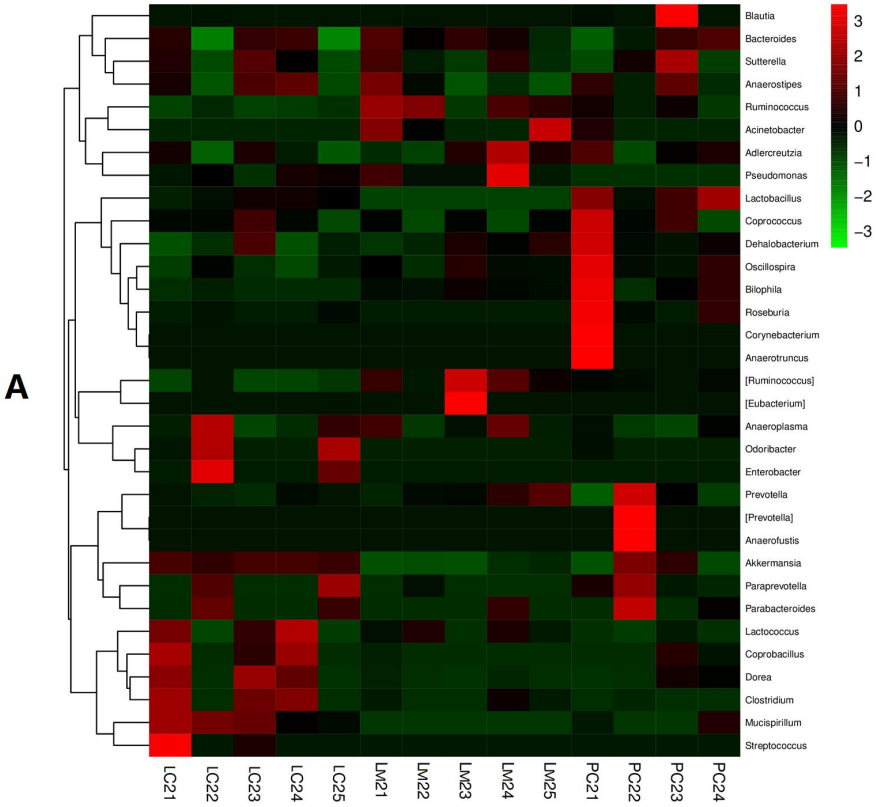

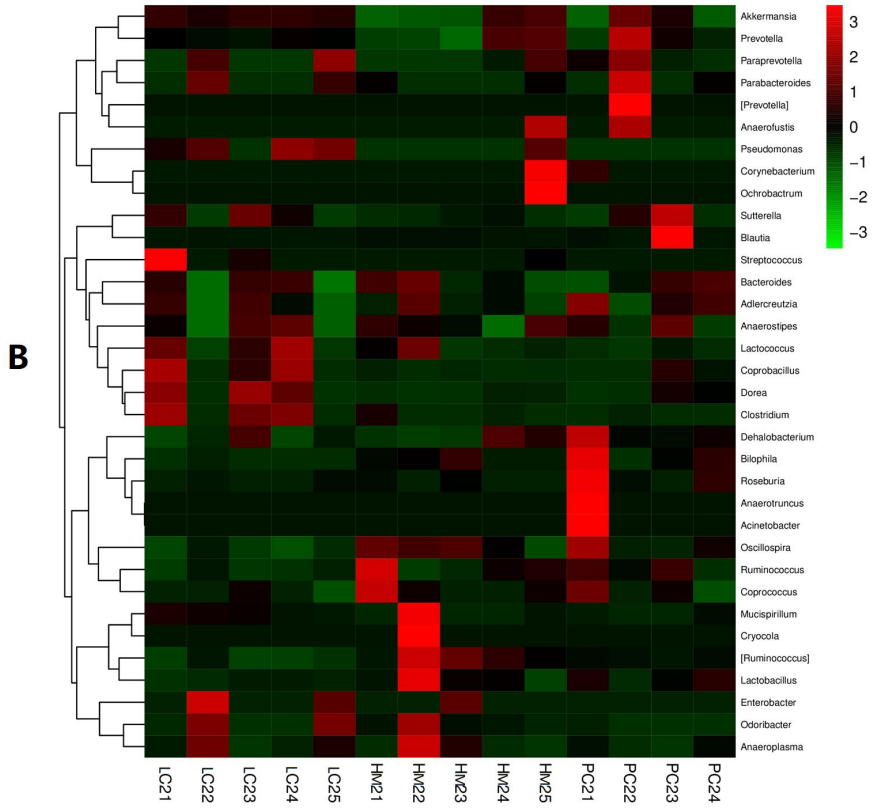

529

530 Figure 8.

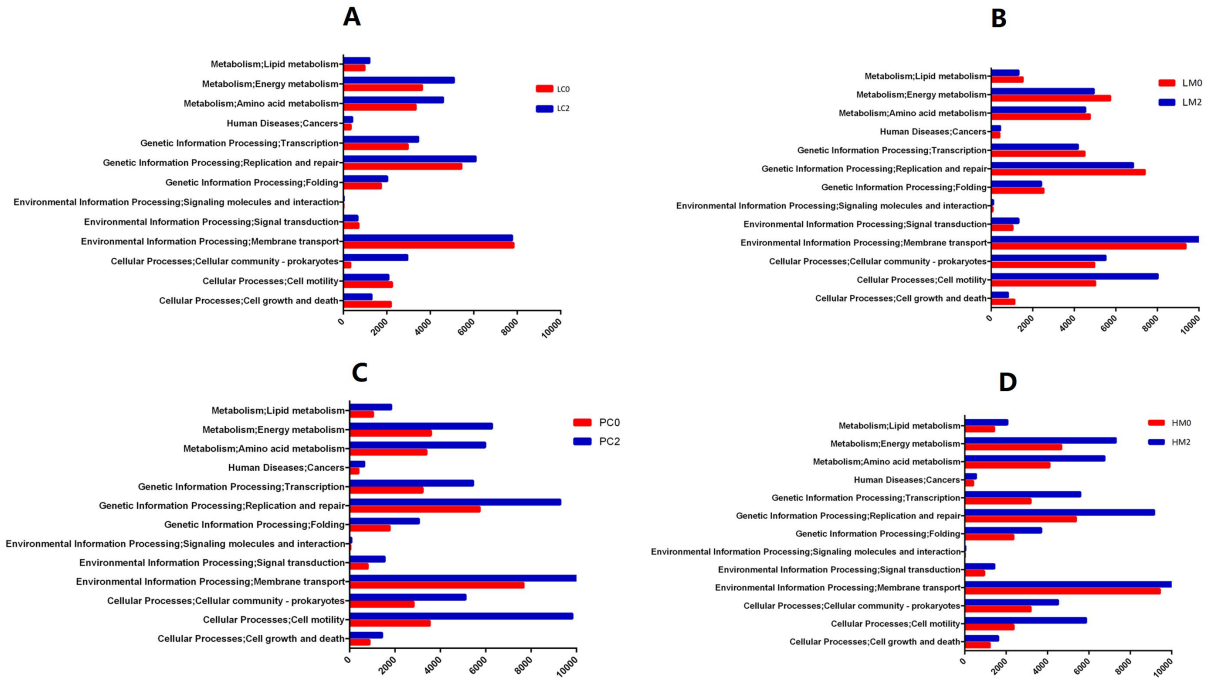

531